

INVESTIGATION OF TRAPPED MAGNETIC FLUX IN SUPERCONDUCTING NIOBIUM SAMPLES WITH NEUTRON RADIOGRAPHY

Oliver Kugeler*, Marc Krzyzagorski, Julia Köszegi, Ralf Ziesche, Luisa Riik,
Tobias Junginger, Jens Knobloch, Wolfgang Treimer
Helmholtz Zentrum Berlin, Albert-Einstein-Straße 15, 12489 Berlin, Germany

Abstract

The dynamics of flux expulsion in Nb samples during superconducting transition has been investigated with neutron radiography. Aiming at a reduction of the trapped flux with respect to obtaining a small residual resistance it was attempted to influence the expulsion by applying external AC magnetic fields. The results of these experiments are presented.

INTRODUCTION

Trapped magnetic flux is a major contribution to the residual resistance of superconducting cavities. Minimizing the trapped flux can significantly reduce operation costs of superconducting CW accelerators. In order to gain a better understanding of the mechanisms, various techniques have been employed to measure it: Field probes like fluxgates [1] or AMR sensors [2] can only indirectly measure the trapped flux, by deducing it from the change in ambient field due to incomplete Meissner transition, taking into consideration the demagnetization behavior of the involved sample [3] or cavity [4]. Magneto-optic methods can visualize trapped flux on a surface at good resolution better than $10\text{ }\mu\text{m}$ [5–7]. We present a complimentary method, polarized neutron radiography [8–10], which measures the field directly and provides spatially resolved in-depth information from the entire volume of the investigated sample. We apply this method to the specific questions of SRF applications. The following issues were addressed with radiographies:

- Influence of cool-down speed on the amount of trapped flux
- Influence of applied field on trapped flux
- Influence of an AC external magnetic field on the flux trapping behaviour

EXPERIMENTAL

The presented neutron radiographies were recorded with PONTO II, an instrument of the University of Applied Sciences (Beuth Hochschule für Technik) Berlin that is operated at the BER II research reactor at HZB. PONTO II uses cold, spin-polarized neutrons at adjustable wavelengths of $2.9\text{ \AA} \leq \lambda \leq 4.5\text{ \AA}$. A photograph of the PONTO II experiment is shown in Figure 1.

* oliver.kugeler@helmholtz-berlin.de

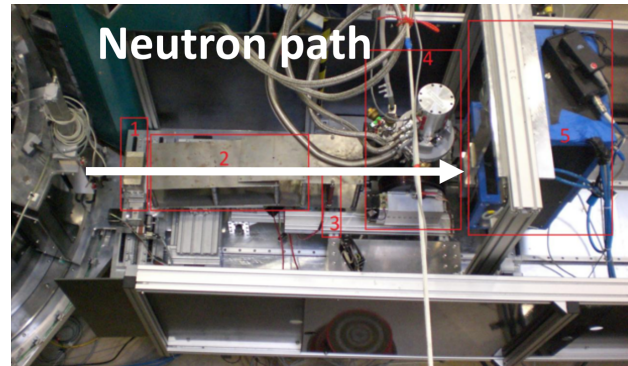


Figure 1: Photograph of the PONTO II set up from top: (1) polarizer, (2) guiding field, (3) spin flipper, (4) sample in cryostat and Helmholtz coils, and (5) neutron detector.

As illustrated in Figure 2, these neutrons are sent through a sample in a closed cycle cryostat that can be cooled down to $T = 4.0\text{ K}$. While there is negligible scattering of neutrons in the setup, their spin interacts only with the ambient magnetic field along the neutron path from the polarizing element, through the sample, up to the analysing element and the detector. A flat field offset measurement with sample in non-superconducting state allows for removing the effects of the inhomogeneous beam, attenuation of sample, sample-holder and temperature shielding and background field. After exposure to the field, neutrons are detected in an up to $40\text{ mm} \times 40\text{ mm}$ field of view at a spatial resolution of $120\text{ }\mu\text{m}$. The phase of the precession due to the amount of magnetic field can be detected by a second polarizer in front of the detector in multiples of 2π .

The samples were cut from a large grain ingot of high purity RRR300 Niobium provided by Heraeus. The obtained cylindrical discs were 5 mm in radius and 5 mm in height. They received a chemical polish at DESY in a beaker. The amount of removed material by the flash (1:1:2) BCP was not monitored. Samples were mounted into an aluminum sample holder with Titanium spring-loaded bolts. The holder is shown in the right part of Figure 3. The holder was installed in the cryostat and conduction cooled via a cold trap. A Helmholtz coil around the cryostat allowed to apply a homogeneous magnetic field during phase transition, see left part of Figure 3. The field cooling was always performed by starting from a stabilized temperature above $T = 15\text{ K}$ above $T_c = 9.2\text{ K}$, then applying a certain cooling rate that could be

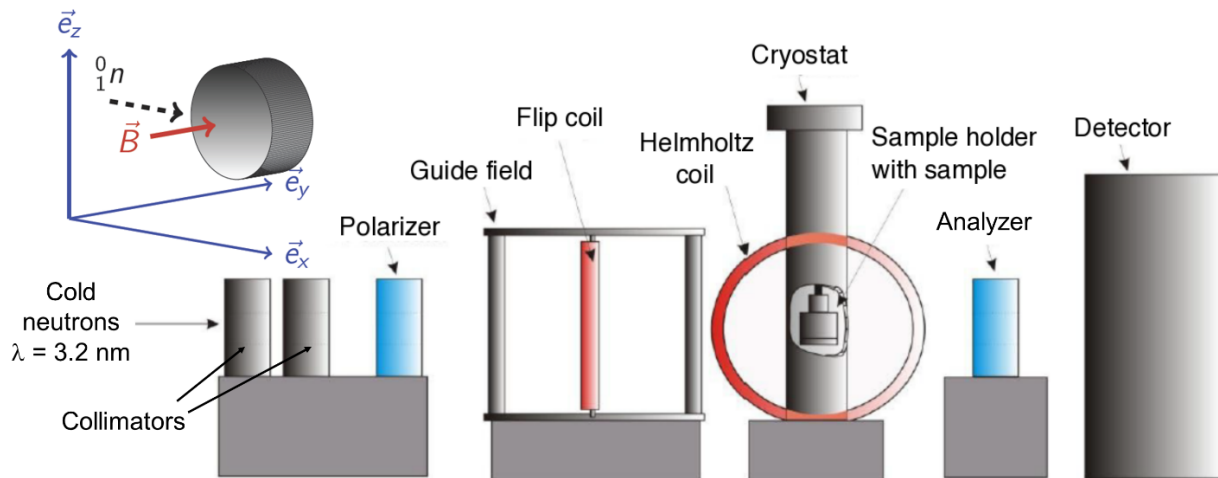


Figure 2: Setup of the PONTO II experiment: Cold neutrons from the HZB reactor BER II reactor are collimated and spin polarized. The neutron trajectory leads through a guide field with the option to perform a spin-flip by a flip-coil, the sample inside a cryostat, and a spin analyzer, and it ends in the detector. The spin rotates in the magnetic field of a sample and hence typically approaches the spin analyzer in a non-parallel orientation. The angle of the final spin rotation depends on the magnetic field along the neutron path. Changes in the polarization reduce the transmission through the spin analyzer which leads to contrast information of the recorded images. The influence of the guide field has to be accounted for with calibration measurements. The inset shows the orientation of sample, neutron velocity and trapped magnetic field, here: 0 ° position).

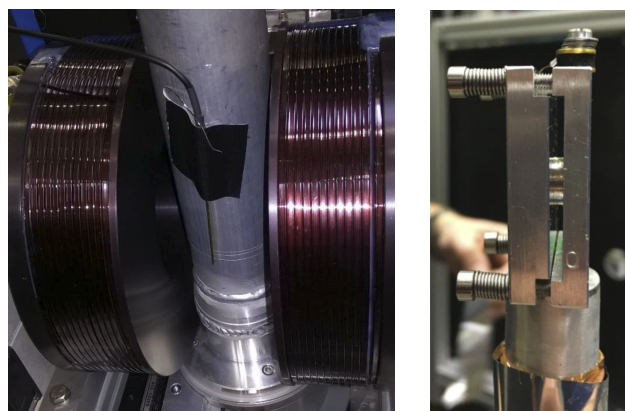


Figure 3: Left: Helmholtz coil used for field cooling of sample in cryostat. Maximum fields of 60 mT (85 mT for a short time) could be generated across the sample. Magnetic fields were measured with a Hall probe. Right: Holding frame and mounted Nb-sample.

varied between 0.1 K/min and 1 K/min. When a temperature of 5 K was reached the external field was turned off. The applied external field was always oriented parallel to the cylinder length axis. The Helmholtz coils could be operated in AC mode up to 10 Hz with arbitrary superposition of DC magnetic field offset. After the sample transitioned into the superconducting state, the coils were turned off, i.e. all

samples in the experiments presented here were field-cooled. Then the magnetic field trapped inside the superconductor was exposed to the neutron beam. In the default position (or 0°-position) the sample-axis and thus the trapped field was oriented perpendicular to the neutron beam. The sample holder could be rotated vertically by 360°. Rotating it by 90 ° brought the sample into a position where its axis was facing and the trapped field was oriented parallel to the neutron beam (90° position). In the tests, the cooling speed was varied between 0.1 K/min and 1 K/min as limited by the cold trap. Also, the ambient field was varied by (a) applying different DC field levels between 0 mT and 5 mT, (b) applying different AC field levels at different frequencies with (c) different superimposed DC offset levels. For each cooling procedure a set of two radiographs in 0° and the complementary 90° position were recorded. Each radiograph required about 4 hours of exposure time.

RESULTS

The analysis and evaluation of neutron data into radiographs is described elsewhere [8]. The following results were obtained: The cooling rate (within the limitations of the cold trap) did not influence the amount of trapped flux. The resulting images at different rates were identical, see Figure 4.

The amount of trapped flux increased linearly with the amount of applied field. Figure 5 shows radiographies obtained after cooling at different ambient, static magnetic

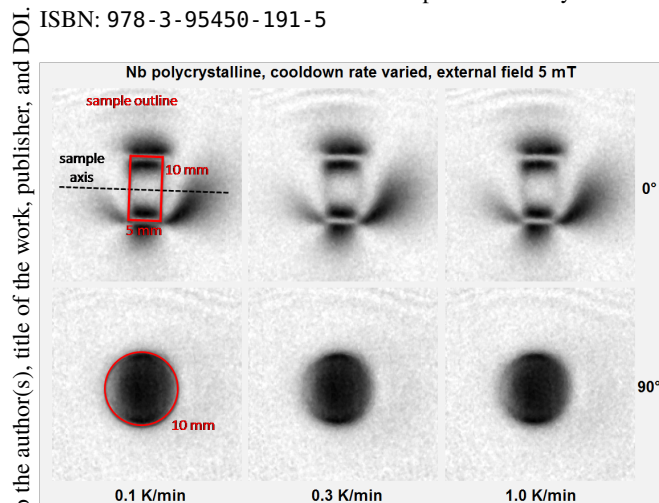


Figure 4: Cooling in external magnetic field of 5 mT at varying rates. The neutron beam is always perpendicular to the paper plane. The sample outline and dimensions are indicated in red. Upper row: 0° sample orientation, lower row: 90° sample orientation.

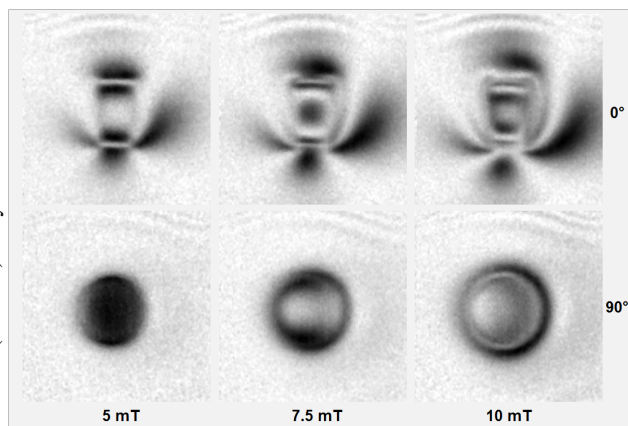


Figure 5: Cooling at various external DC-magnetic fields and cooling rate = 0.3 K/min.

trapping mechanism is inactive since there is no flux line present that could be trapped. The results of those efforts are shown in Figure 6: The sample was field-cooled in different external magnetic fields, 2 mT, 3 mT, and 5 mT, and an AC field with 10 mT amplitude was superimposed at 0.1 Hz, and 0.5 Hz. The measured spin-polarization in the sample-center is plotted in the right graphs. The result of these expulsion attempts is that less flux is trapped at higher frequencies under otherwise identical conditions. From the spin-flip data in Figure 6 this effect can be converted to approximately 20% less trapping when going from 0.1 Hz to 0.5 Hz. The series could not be continued to even higher frequencies due to dielectric heating at the cryostat, so the results are not significant enough to make a solid statement. Also, in order to be usable as a flux removal procedure one would aim at 100% efficiency rather than the observed effect.

CONCLUSION

The flux trapping and expulsion behavior of field-cooled samples has been investigated with neutron tomography. The amount of trapped flux was proportional to the external field and independent on cooling rate. The trapping efficiency seems to decrease with the frequency of a superimposed external AC magnetic field.

REFERENCES

- [1] S. Aull, O. Kugeler, and J. Knobloch, "Trapped magnetic flux in superconducting niobium samples," *Physical Review Special Topics - Accelerators and Beams*, vol. 15, pp. 1-6, 2012.
- [2] B. Schmitz, K. Alomari, O. Kugeler, J. Köszegi, Y. Tamaševich, and J. Knobloch, "Setup of a spatially resolving vector magnetometry system for the investigation of flux trapping in superconducting cavities," in *Proc. IPAC2017*, Copenhagen, Denmark, <https://doi.org/10.18429/JACoW-IPAC2017-MOPVA050>, 2017.
- [3] S. Aull, *Investigation of trapped magnetic flux in superconducting niobium samples*, Thesis, 2011.
- [4] A. Romanenko, A. Grassellino, A. C. Crawford, D. A. Serfaty, and O. Melnychuk, "Ultra-high quality factors in superconducting niobium cavities in ambient magnetic fields up to 190 mg," [arXiv:1410.7877v1](https://arxiv.org/abs/1410.7877v1), 2014.
- [5] L. Vinnikov and A. Golubok, "Direct observation of magnetic structure in niobium single crystals with hydride precipitate pinning centres," *Phys. Stat. Sol. (a)*, vol. 69, p. 631, 1982.
- [6] A. Polyanskii, V. Beilin, M. Feldmann, M. Roth, E. Hellstrom, and D. Larbalestier, "Magneto-Optical Investigation of Superconducting Materials", *Magneto-Optical Investigation of Superconducting Materials*, vol. 142, pp. 19-28. https://doi.org/10.1007/978-94-007-1007-8_3, 2005.
- [7] A. A. Polyanskii, P. J. Lee, A. Gurevich, Z.-H. Sung, and D. C. Larbalestier, "Magneto-Optical Study High-Purity Niobium for Superconducting RF Application," in *Symposium on the Superconducting Science and Technology of Ingot Niobium*, AIP Conf. Proc., 1352, <https://doi.org/10.1109/TASC.2009.2017762>, 2011.

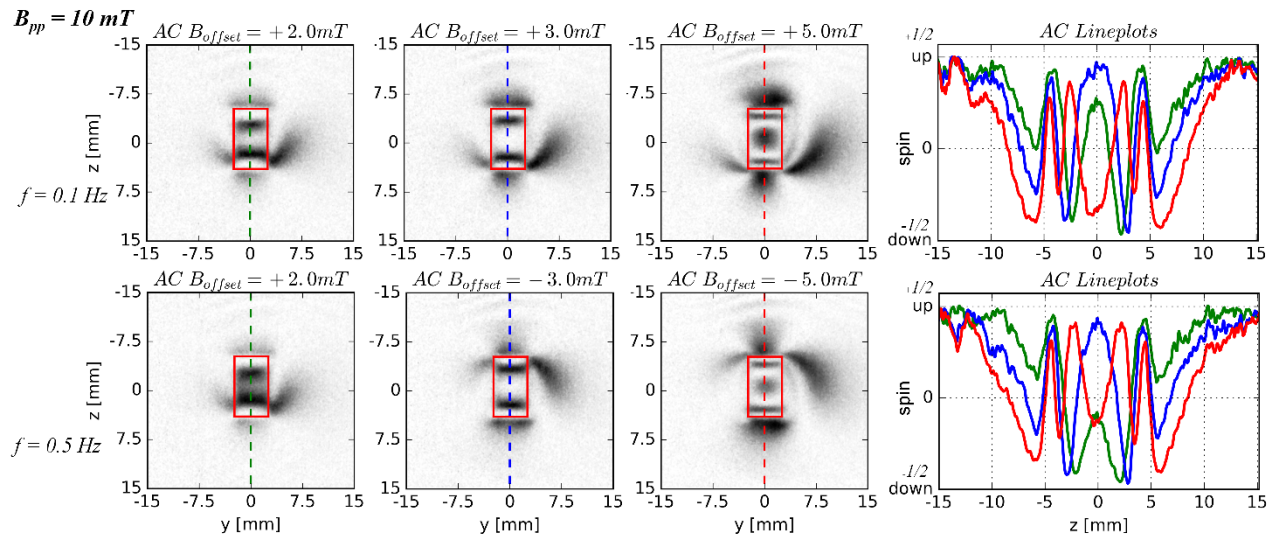


Figure 6: Radiographs of ac-field cooled sample. The field amplitude was always 10 mT peak to peak. The DC offset field and the frequency of the AC field were varied. The right graphs show the integrated spin phase change.

- [8] N. Kardjilov, I. Manke, M. Strobl, A. Hilger, W. Treimer, M. Meissner, T. Krist, and J. Banhart, "Three-dimensional imaging of magnetic fields with polarized neutrons," *Nature Physics*, vol. 4, pp. 399–403, 2008.
Physical Review B, vol. 85, <https://doi.org/10.1103/PhysRevB.85.184522>, 2012.
- [9] W. Treimer, O. Ebrahimi, N. Karakas, and R. Prozorov, "Polarized neutron imaging and three-dimensional calculation of magnetic flux trapping in bulk of superconductors," *Physics Procedia*, vol. 43, pp. 243–253, <https://doi.org/10.1016/j.phpro.2013.03.028>, 2013.